Proceedings of 20th International Congress on Acoustics, ICA 2010

23-27 August 2010, Sydney, Australia

Design considerations in an automatic classification system for bird calls using the Two-dimensional Geometric Distance and cluster analysis

Michihiro Jinnai (1), Neil J Boucher (2), Jeremy Robertson (3), and Sonia Kleindorfer (4)

(1) Kagawa National College of Technology, Takamatsu, Kagawa, Japan jinnai@t.kagawa-nct.ac.jp
(2) SoundID, Maleny, Queensland, Australia nboucher@ozemail.com.au
(3) School of Biological Sciences, Flinders University, Adelaide, Australia jeremy.robertson@flinders.edu.au
(4) School of Biological Sciences, Flinders University, Adelaide, Australia sonia.kleindorfer@flinders.edu.au

PACS: 43.80.-n Bioacoustics

ABSTRACT

We have been developing an automatic classification system for bird calls. Many biologists have been using the early one-dimensional version of our system and we have been working on a two-dimensional method. The software extracts a sonogram from the bird call using the LPC spectrum analysis and classifies the images of sonogram using a similarity scale and cluster analysis. We use the new similarity scale called the "Two-dimensional Geometric Distance" that has been developed by Jinnai and Boucher. In this paper, we introduce the principles of the Two-dimensional Geometric Distance, demonstrate the two-dimensional pattern matching software, and describe design considerations in a new automatic classification system for bird calls. Testing has shown an order of magnitude improvement in accuracy over the one-dimensional method.

1. INTRODUCTION

We have developed an automatic classification system for bird calls over the past seven years. In general, when a human researcher classifies bird calls manually, two methods are used as follows. In the first method, the researcher compares the bird calls by simply listening to them; a small number of experts are very good at this, but most researchers are not. In the second method, the sound spectrum patterns are extracted from bird calls using the FFT spectrum analysis and others, and the researcher compares these images to classify them by sight. In both cases, human researchers become fatigued after about 20 minutes, which limits the duration of effective concentration. In order to automate this process, we have been developing software that: (1) extracts sonograms from bird calls using the LPC spectrum analysis, (2) matches images of the sonogram using a similarity scale, and (3) classifies the bird calls using cluster analysis.

The similarity scale works as follows: for calls for which a researcher would recognize two patterns as similar to each other, the computer software outputs a small value, and for calls for which a researcher would recognize the two patterns as dissimilar, then the computer software outputs a large value. In conventional cluster analysis, the similarity scales known as the Euclidean distance and cosine similarity are widely used to measure likeness. Conventional similarity scales compare the patterns using one-to-one mapping. The result of the one-to-one mapping is that the distance metric is highly sensitive to noise, and the distance metric changes in a staircase pattern when a difference occurs between peaks of the standard and input patterns.

As an improvement, we have developed a new similarity scale called the Geometric Distance [11]. We have been developing the automatic classification software for bird calls (and other sounds) using the Geometric Distance. As of early 2010, we have commercial software that extracts LPC spectrum patterns (frequency-power) from bird calls (or other sounds), and classifies them using One-dimensional Geometric Distance (1-d GD) [2]. We have now moved on to a method that extracts sonograms (time-frequency-power) from the bird calls, and processes them using Two-dimensional Geometric Distance (2-d GD). From experimental testing, we have found that the 1-d GD performed significantly better than the Euclidean distance and cosine similarity, and that the 2-d GD performed significantly better than the 1-d GD.

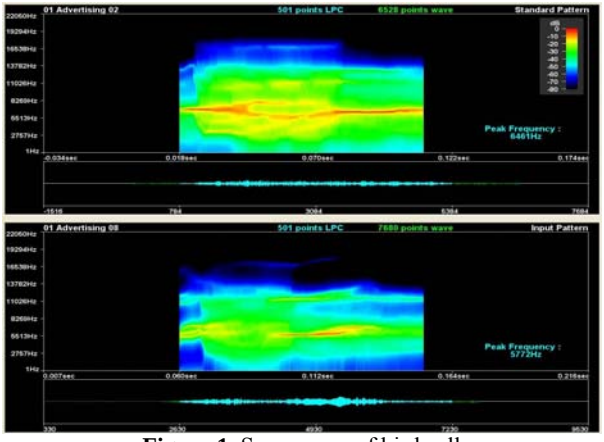

Figure 1. Sonograms of bird call

In this paper, we introduce the principles of the 2-d GD, demonstrate the two-dimensional pattern matching software, and describe design considerations in a new automatic classification system for bird calls using the 2-d GD and cluster analysis. Moreover, we describe the biological significance.

2. THE SONOGRAM OF BIRD CALLS

Figure 1 shows the sonograms (time-frequency-power) extracted from the calls of the critically endangered bird Coxen's Fig-Parrot (*Cyclopsitta diophthalma coxeni*). These sonograms have been calculated using the method of Linear Predictive Coefficient (LPC). We have set the analysis conditions of the bird call with the 44.1kHz sampling frequency, 16 bit quantization, 11.4 msec frame width, 0.23 msec frame period, 441 total frames, 16 order LPC, 1Hz to 22050Hz frequency range, 86Hz frequency resolution, and −80dB to 0dB logarithmic power spectrum.

From the upper and lower sonograms shown in Figure 1, it is evident that the peak frequencies are 6461Hz and 5772Hz respectively and the two patterns are not similar to each other. Moreover, as a result of comparing these two bird calls aurally, we have confirmed that these two calls are not similar to each other. The software registers the similarity or Geometric Distance as 4.2 degrees. Identical calls would register a distance of zero degrees, whereas reasonably similar calls might register from 1.0 to 3.5 degrees.

3. THE SIMILARITY SCALE AND ITS ROBUSTNESS

From studies already done we have determined that in the case of bird calls, not two calls are sufficiently alike, that the software using the conventional similarity scales cannot distinguish between them. Even in the instance where a given bird produces a string of seemingly repetitive calls, there are subtle differences that can be detected. Variability of calls between individuals and groups geographically removed are even wider. It is necessary therefore to have a method that can cope with this variation and still recognize the similarity of the calls.

Additionally in the recording process there will be noise (often substantial) and distortion from various sources. In this section we examine how the method deals with discrete variations and show that it is robust under the expected variability's that might be encountered.

In sound recognition, a known sonogram stored in a PC memory is called here the "standard pattern", and a comparison sonogram is called "input pattern". The degree of likeness between the standard pattern and the input pattern is evaluated using a similarity scale. If the similarity of the standard and input patterns is close, then those two patterns are considered to be in the same category and the input pattern is recognized and classified. The similarity is often measured as a "distance" between the two patterns. Conventionally, the similarity scales known as the Euclidean distance and cosine similarity have been widely used. Section 3.1 describes the shortcomings that are found in the conventional similarity scales. Furthermore, Sections 3.2 and 3.3 describe new similarity scales called the "One-dimensional Geometric Distance (1-d GD)" and the "Two-dimensional Geometric Distance (2-d GD)" that have been developed by Jinnai and Boucher for improving the shortcomings.

3.1. Euclidean distance and cosine similarity —Conventional similarity scale

Conventional similarity scales Euclidean distance and cosine similarity compare the patterns using one-to-one mapping. The result of the one-to-one mapping is that input patterns with different shapes may have the same distance from the standard pattern when the sonograms have the "difference" and "wobble".

The upper diagram of Figure 2 shows an example of the "difference" where the standard pattern has two peaks in the sonogram, and input patterns 1, 2, and 3 have a different position on the first peak. Note that the standard and input patterns have the same volume. As shown in the bar graph at the bottom left of Figure 2, the Euclidean distances and cosine similarities e_1, e_2, and e_3 have the relationship of $e_1=e_2=e_3$ between the standard pattern and each of input patterns 1, 2, and 3. Therefore, input patterns 1, 2, and 3 cannot be distinguished.

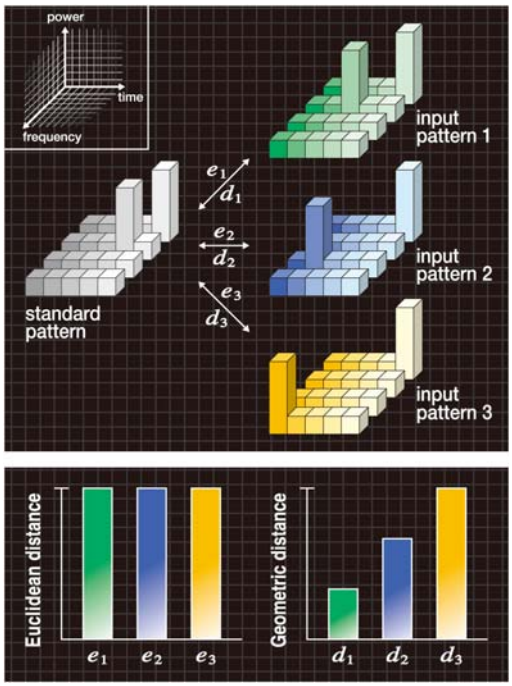

Figure 2. Typical example of "difference"

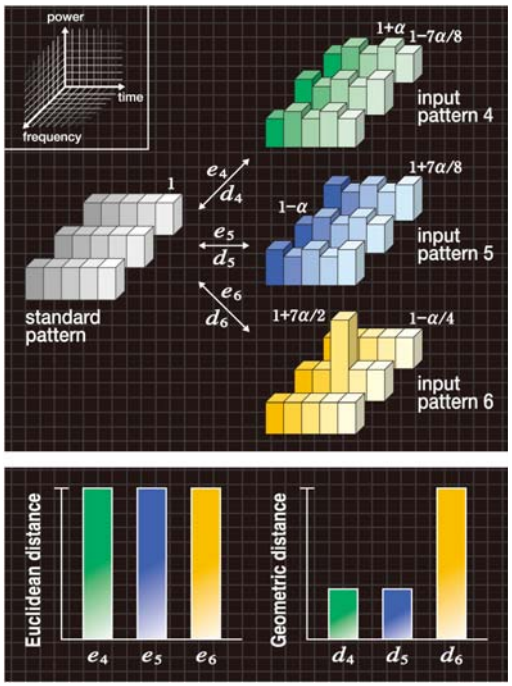

Figure 3. Typical example of "wobble"

The upper diagram of Figure 3 shows an example of the "wobble" where the standard pattern has a flat sonogram, input patterns 4 and 5 have the "wobble" on the flat sonogram, and input pattern 6 has a single peak. However, each pattern is assumed to have variable α in the relationship shown in Figure 3. Therefore, the standard and input patterns always have the same volume. As shown in the bar graph at the bottom left of Figure 3, the Euclidean distances and cosine similarities e_4, e_5, and e_6 have the relationship of $e_4=e_5=e_6$ between the standard pattern and each of input patterns 4, 5, and 6. Therefore, input patterns 4, 5, and 6 cannot be distinguished.

3.2. One-dimensional geometric distance

As an improvement, we have developed a new similarity scale called the Geometric Distance [11]. A similarity scale is a concept that should intuitively concur with the human concept of similarity in hearing and sight. First we need to develop a mathematical model for the similarity scale so that we can perform numerical processing by computation. In the Geometric Distance, a mathematical model of the similarity scale is proposed to improve the shortcomings that are found in the Euclidean distance, cosine similarity and others. A mathematical model incorporating the following two characteristics is used.

< 1 > The distance metric must show good immunity to noise.

< 2 > The distance metric must increase monotonically when a difference increases between peaks of the standard and input patterns.

The bar graphs at the bottom right of Figures 2 and 3 express the mathematical model by figures. Following on from above, a new algorithm based on one-to-many point mapping is proposed to realize the mathematical model. This section describes the 1-d GD algorithm.

Figures 4(a)–(e) respectively show typical examples of the standard and input patterns that have been created using the momentary power spectrum (frequency-power) of standard and input sounds. Note that the power spectrum is generated from the output of filter bank with the m frequency bands. The i-th power spectrum values (where, i = 1, 2, … , m) are divided by their total energy, so that normalized power spectra s_i and x_i have been calculated. At this moment, the standard and input patterns have the same area size. Moreover, Figures 4(a)–(e) respectively show reference patterns that have the initial shape r_i of a normal distribution.

With the 1-d GD algorithm, a difference in shapes between standard and input patterns is replaced by the shape change of the reference pattern using the following equation.

$$r_i \longleftarrow r_i + (x_i - s_i) \qquad (i = 1, 2, 3, \cdots, m) \tag{1}$$

Next, we explain Eq. (1) using Figure 4.

- Figure 4(a) gives an example of the case where standard pattern and input pattern have the same shape. Because values r_i of Eq. (1) do not change during this time, the reference pattern shown in Figure 4(a) do not change in the shape from the normal distribution.
- Figures 4(b)–(d) respectively show examples exhibiting a small, medium, and large "difference" of peaks between the standard and input patterns. If Eq. (1) is represented by the shapes, as shown in Figures 4(b)–(d), value r_i decreases at peak position i of each standard pattern. At the same time, value r_i increases at peak position i of each input pattern.

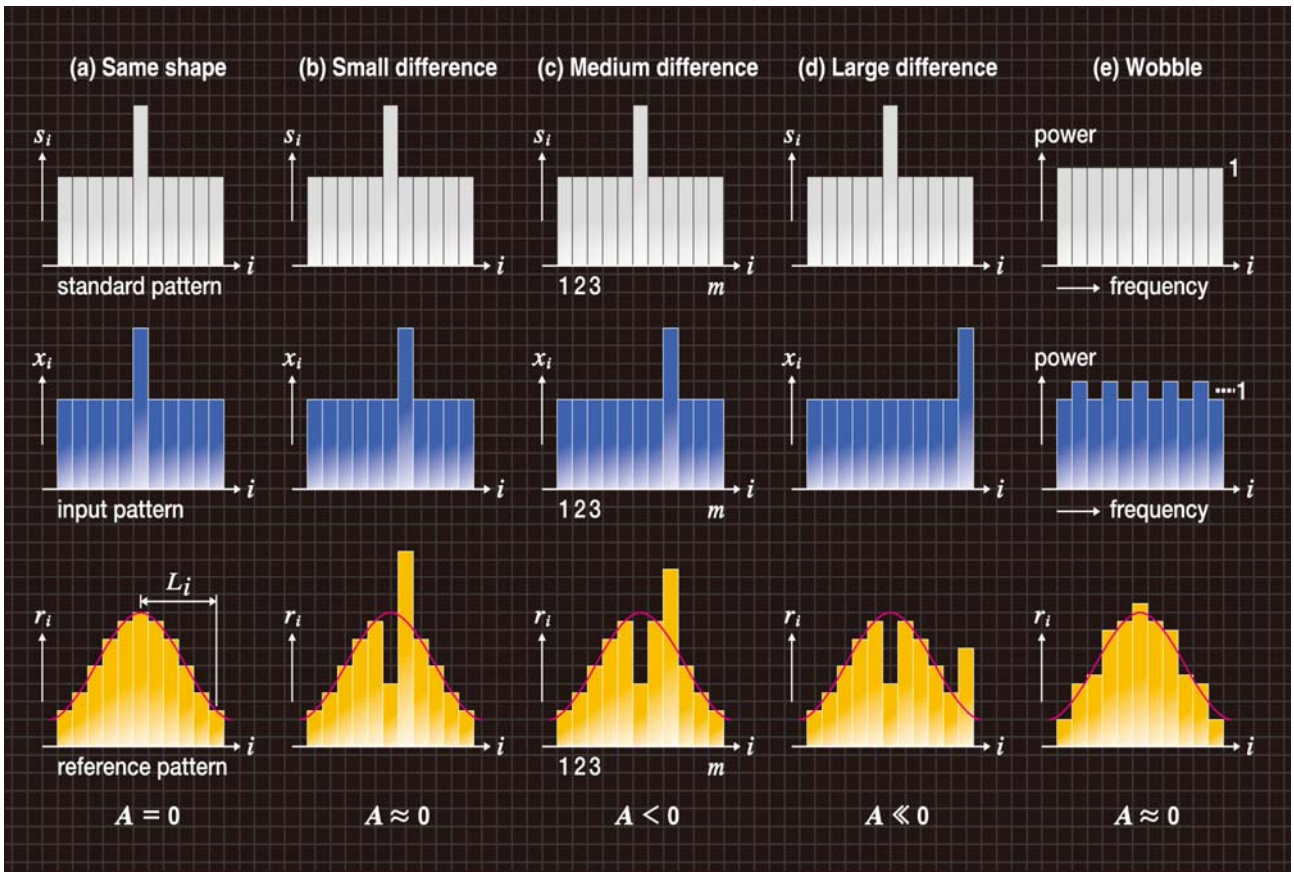

Figure 4. Shape changes of reference patterns

● Figure 4(e) typically shows the standard pattern having a flat shape and the input pattern where a "wobble" occurs in the flat shape. Because values r_i increase and decrease alternatively in Eq. (1) during this time, the reference pattern shown in Figure 4(e) has a small shape change from the normal distribution.

For the reference pattern whose shape has changed by Eq. (1), the magnitude of shape change is numerically evaluated as the variable of moment ratio. The moment ratio of the reference pattern can be calculated using the following equation.

$$A = \frac{\left\{\sum_{i=1}^{m} r_i\right\} \cdot \left\{\sum_{i=1}^{m} (L_i)^4 \cdot r_i\right\}}{\left\{\sum_{i=1}^{m} (L_i)^2 \cdot r_i\right\}^2} - 3 \qquad (2)$$

Where, L_i (i = 1, 2, … , m) is a deviation from the center axis of the normal distribution as shown in the reference pattern of Figure 4(a). The moment ratio A is derived from the kurtosis from a statistical analysis. If the shape of the reference pattern follows the normal distribution, then $A = 0$. If it has peakedness relative to the normal distribution, then $A > 0$. Alternatively, if it has flatness relative to the normal distribution, then $A < 0$. Figures 4(a)–(e) show how A varies with r_i.

● In Figure 4(a), the value r_i do not change. The moment ratio becomes $A = 0$.

● In Figure 4(b), the position i of the decreased r_i and that of the increased r_i are close. Because the effect of an increase and a decrease is canceled out, the moment ratio becomes $A \approx 0$.

● In Figure 4(d), because the shape of reference pattern has flatness relative to the normal distribution, the moment ratio becomes $A \ll 0$.

● In Figure 4(c), because the shape of the reference pattern is an intermediate state between (b) and (d), the moment ratio becomes $A < 0$.

● In Figure 4(e), the reference pattern has small shape change from the normal distribution, and the moment ratio becomes $A \approx 0$.

From Figures 4(a)–(d), we can understand that value $|A|$ increases monotonically according to the increase of the "difference" between peaks of the standard and input patterns. Also, from Figure 4(e), it is clear that $A \approx 0$ for the "wobble".

As shown in Figure 4, we have determined the moment ratio A by assuming that the center axis of the normal distribution locates at the center of standard and input patterns. Next, as shown in Figure 5, we determine the amount of moment ratio A_j for each j in the case where the center axis of the normal distribution moves to any component position j (where, j = 1, 2, … , m) of the standard and input patterns. Using the m parts of the moment ratio A_j that we have obtained in Figure 5, we can calculate the difference in shapes between standard and input patterns by the following equation and we define it as the "One-dimensional Geometric distance d".

$$d = \sqrt{\sum_{j=1}^{m} (A_j)^2} \qquad (3)$$

In this method, when a "difference" occurs between peaks of the standard and input patterns with a "wobble" due to noise or other non-linearity, the "wobble" is absorbed and the distance metric increases monotonically according to the increase of the "difference". From the above description, we could verify that the 1-d GD algorithm matches the characteristics <1> and <2> of the mathematical model. In the actual 1-d GD algorithm, we create a pair of reference patterns that have the initial shape of the normal distribution, because Eq. (2) cannot be defined if the value r_i is negative [11].

3.3. Two-dimensional geometric distance —New similarity scale

The 1-d GD algorithm is expanded to the 2-d GD algorithm. Figures 6 and 7 respectively show stylized examples of the standard and input patterns that have been created using the sonogram (time-frequency-power) of standard and input sounds. The (i_1, i_2)-th power spectrum values (where, time axis i_1 = 1, 2, … , m_1; frequency axis i_2 = 1, 2, … , m_2) are divided by their total energy, so that normalized power spectra $s_{i_1 i_2}$ and $x_{i_1 i_2}$ have been calculated. At this moment, the standard and input patterns have the same volume size. Moreover, Figures 6 and 7 respectively show reference patterns that have the initial shape $r_{i_1 i_2}$ of a two-dimensional normal distribution.

Figure 6 shows an example exhibiting a "difference" of peaks between the standard and input patterns. Figure 7 shows the standard pattern having a flat shape and the input pattern where a "wobble" occurs in the flat shape. We suppose that the standard and input patterns have the same volume. With the 2-d GD algorithm, a difference in shapes between standard and input patterns is replaced by the shape change of the reference pattern using the following equation.

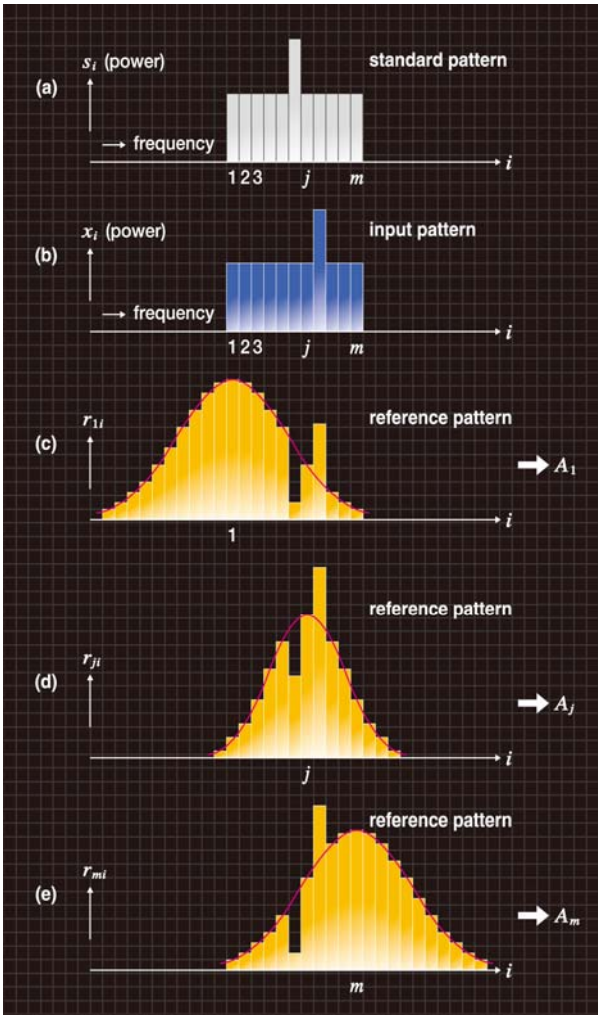

Figure 5. Movement of reference pattern

$$r_{i_1 i_2} \longleftarrow r_{i_1 i_2} + (x_{i_1 i_2} - s_{i_1 i_2}) \quad \begin{matrix} (i_1 = 1, 2, 3, \cdots, m_1) \\ (i_2 = 1, 2, 3, \cdots, m_2) \end{matrix} \tag{4}$$

In Figure 6, the value of the reference pattern decreases at peak position of the standard pattern. At the same time, the value of the reference pattern increases at peak position of the input pattern. In Figure 7, because the values of the reference pattern increase and decrease alternatively, the reference pattern has a small shape change from the two-dimensional normal distribution.

For the reference pattern whose shape has changed by Eq. (4), the magnitude of shape change is numerically evaluated as the variable of moment ratio using the following equation.

$$A = \frac{\left\{\sum_{i_1=1}^{m_1}\sum_{i_2=1}^{m_2} r_{i_1 i_2}\right\}\cdot\left\{\sum_{i_1=1}^{m_1}\sum_{i_2=1}^{m_2} (L_{i_1 i_2})^4 \cdot r_{i_1 i_2}\right\}}{\left\{\sum_{i_1=1}^{m_1}\sum_{i_2=1}^{m_2} (L_{i_1 i_2})^2 \cdot r_{i_1 i_2}\right\}^2} - 3 \tag{5}$$

However, the deviation L_i shown in Figure 4(a) and Eq. (2) is replaced by a deviation $L_{i_1 i_2}$ shown in Figure 6.

Next, as shown in Figure 8, we determine the amount of moment ratio $A_{j_1 j_2}$ for each (j_1, j_2) in the case where the center axis of the two-dimensional normal distribution moves to various positions (j_1, j_2) relative to the standard and input patterns. Using these moment ratios $A_{j_1 j_2}$, we can calculate the difference in shapes between standard and input patterns by the following equation and we define it as the "Two-dimensional Geometric Distance d".

$$d = \sqrt{\sum_{j_1=1}^{m_1}\sum_{j_2=1}^{m_2} (A_{j_1 j_2})^2} \tag{6}$$

Also, we can verify that the 2-d GD algorithm matches the characteristics <1> and <2> of the mathematical model.

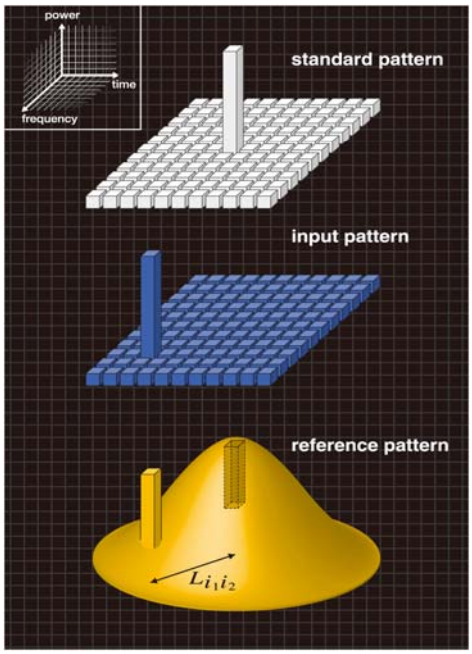

Figure 6. Shape change of reference pattern (difference)

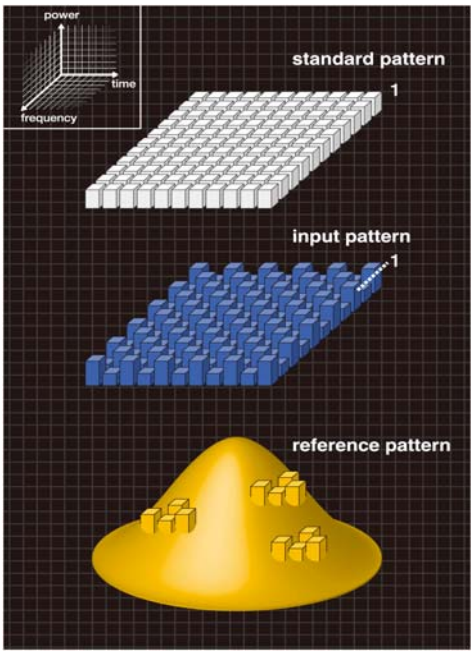

Figure 7. Shape change of reference pattern (wobble)

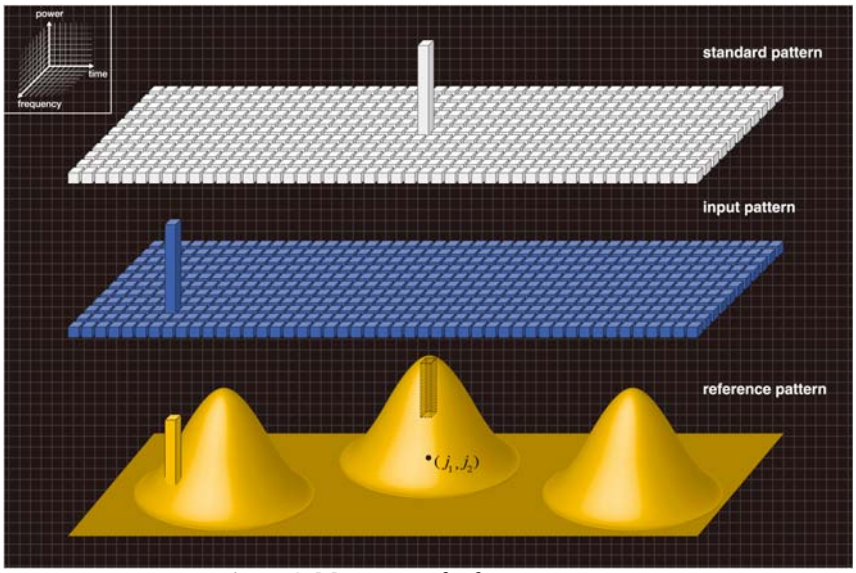

Figure 8. Movement of reference pattern

4. AUTOMATIC CLASSIFICATION FOR BIRD CALLS

Figure 9 shows a concept of the cluster analysis. The similar images are classified into the same cluster using a similarity scale. In conventional cluster analysis, the similarity scales known as the Euclidean distance and cosine similarity are widely used to measure likeness. In this paper, we perform the cluster analysis using the 2-d GD instead of the conventional similarity scales.

We suppose that the N sonograms are extracted from the N bird calls and that the M clusters are obtained after classification, where $N > M$. In our system, we perform cluster analysis with the following processing procedure to classify the bird calls automatically.

(Step 1) The value d_{ij} of the 2-d GD is calculated between the i-th sonogram (i = 1, 2, … , N−1) and the j-th sonogram ($j = i+1, \dots, N$). We obtain the ${}_N C_2$ pieces of the values d_{ij} of the 2-d GD and classify the set (sonogram i, sonogram j) that has the minimum distance value d_{ij} into one cluster. As the result, we have the N−1 clusters.

(Step 2) As shown in Figure 10, if the cluster k and the cluster l have the n_k and n_l sonograms, respectively, then we define a distance $\hat{d}_{kl}$ between these two "clusters" by the following equation.

$$\hat{d}_{kl} = \frac{\sum_{i_k=1}^{n_k} \sum_{i_l=1}^{n_l} d_{i_k i_l}}{n_k n_l} \qquad (7)$$

Note that $d_{i_k i_l}$ is the value of the 2-d GD between the sonogram i_k (i_k = 1, 2, … , n_k) in the cluster k and the sonogram i_l (i_l = 1, 2, … , n_l) in the cluster l. As shown in the left diagram of Figure 11, the distances $\hat{d}_{kl}$ are calculated in each combination of the clusters by using Eq. (7). As shown in the right diagram of Figure 11, we classify the set (cluster k, cluster l) that has the minimum distance value $\hat{d}_{kl}$ into one cluster.

(Step 3) The process of Step 2 is repeated. If we have the M clusters, then we end the process.

By using the above processing procedure, the similar sonograms of the bird calls are classified into the same cluster.

5. THE BIOLOGICAL SIGNIFICANCE OF RELIABLE CLASSIFICATION OF VOCALISATION BEHAVIOUR

Animal vocalisation behaviour plays a key role in evolutionary processes including species recognition and mate attraction (discussed in Collins 2004; Gerhardt & Bee 2006). Furthermore, in animals like song birds and crickets, there are frequently dialects or micro-geographic variation in vocalisation behaviour (Rothstein & Fleischer 1987; Simmons et al. 2001; Zuk et al. 2001; Catchpole & Slater 2008; Colombelli-Négrel 2008; Colombelli-Négrel et al. in press). These dialects may facilitate recognition among individuals of a local population that are adapted to a particular habitat and are genetically distinct from neighbouring populations (genetic adaptation hypothesis: Payne 1981; Rothstein & Fleischer 1987; Simmons et al. 2001; Zuk et al. 2001; Slabbekoorn & Smith 2002, Nicholls & Goldizen 2006). The characteristics of acoustic signals also provide vital cues for mate choice in

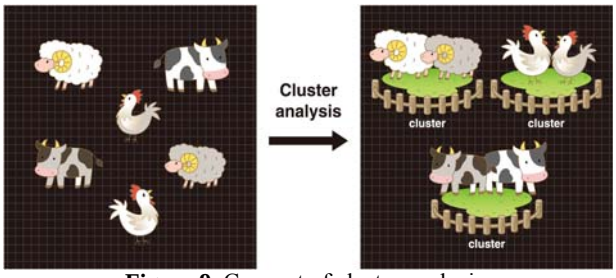

Figure 9. Concept of cluster analysis

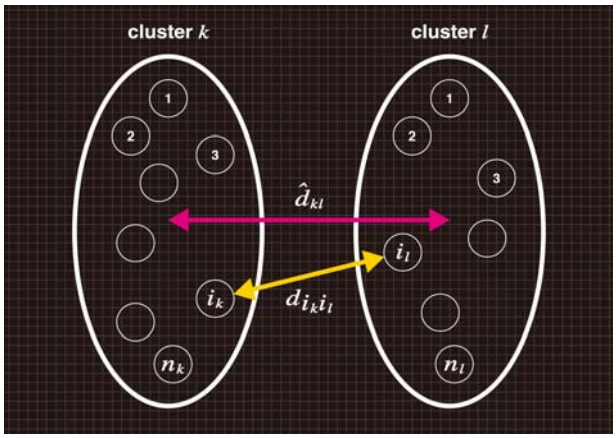

Figure 10. Distance between two "clusters"

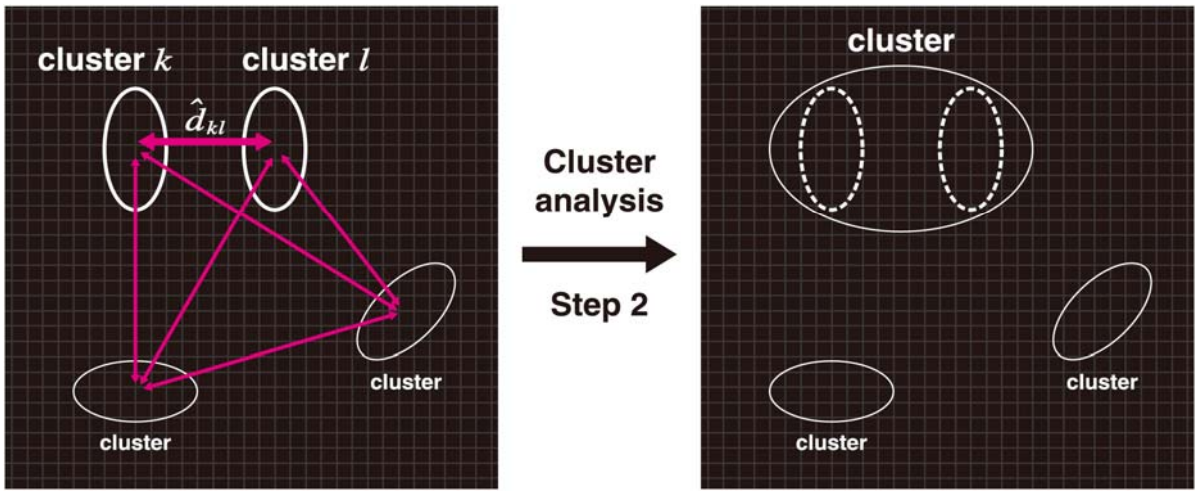

Figure 11. Combination of two clusters

sexual selection (Nottebohm and Selander 1974, Appeltants et al. 2005, Catchpole & Slater 2008). For example, numerous studies have shown the role of acoustic signals in mate choice in crickets (Simmons et al. 2001; Simmons 2004; Scheuber et al. 2004), frogs (Gerhardt 1986, Robertson 1986, 1990; Klump et al. 2004, Gerhardt 2005, Gerhardt & Bee 2006), birds (McGregor & Krebs 1982, Patten et al. 2004) and mammals (Charlton et al. 2007). Acoustic signals can reliably indicate the immune function of the caller in crickets and birds (Simmons et al. 2005; Tregenza et al. 2006, Markman et al. 2008). There is also compelling evidence that this sexual selection for acoustic signals can drive speciation in birds (Seddon et al. 2008). In summary, given the importance of vocalisation behaviour for understanding evolutionary patterns and processes, it is key that we apply reliable methods free from observer bias to interpret bird calls and other forms of vocalisation behaviour.

6. CONCLUSIONS AND FUTURE WORK

We have proposed a new automatic classification system for bird calls. This software extracts the sonogram from the bird call using the LPC spectrum analysis, and matches the images of the sonogram between a standard and an input bird calls using the 2-d GD. Then, the software classifies the bird calls using cluster analysis. We expect that this will result in faster classification and better classification than that which can be achieved by a human expert, especially given that the 1-d method has already proven itself to be comparable to a human expert.

Finally, we describe future work. We will continue to develop commercial software that can be applied to various types of animal calls, human voice and other sounds. We will carry out the classification experiments using various types of sounds and will verify the effectiveness of the proposed method.

REFERENCES

1 Appeltants D, Gentner TQ, Hulse SH, Balthazart J, Ball GF, "The effect of auditory distractors on song discrimination in male canaries (Serinus canaria)", *Behav Processes*, 69, 331-341 (2005)

2 **Boucher NJ**, Burbidge A. and **Jinnai M.**, "Computer recognition of sounds that have never been heard before" *Australian Institute of Physics 18th National Congress*, 211, (2008) **http://www.soundid.net/**

3 Catchpole, C.K. Slater, P.J.B. 2008. Bird Song: Biological Themes and Variations", *Cambridge*, (2008)

4 Charlton BD, Reby D, McComb K, "Female red deer prefer the roars of larger males", *Biol Lett* ***3***, 382-385 (2007)

5 Collins S., "In: Marler & Slabberkorn (Eds) Nature's music", *The Science of Birdsong*, Elsevier Academic Press, (2004).

6 Colombelli-Négrel D, "The evolution of anti-predator responses and vocal communication in superb fairy-wrens (Malurus cyaneus)", *PhD thesis*, (2008)

7 Colombelli-Négrel D., **Robertson J.** and **Kleindorfer S.** (in review), "Risky revelations: A unique bird song that warns of danger and identifies the singer", *Journal of Ornithology*

8 Gerhardt HC, "Evolutionary and neurobiological implications of selective phonotaxis in the green Treefrog", *Hyla cinerea, Exp Biol*, 45, 167-178 (1986)

9 Gerhardt HC, "Advertisement-Call Preferences in Diploid-Tetraploid Treefrogs (Hyla chrysoscelis and Hyla versicolor)", *Implications for Mate Choice and the Evolution of Communication Systems, Evolution* 59, 395-408 (2005)

10 Gerhardt, H.C. & Bee A. Bee, "In: Hearing and Sound Communication in Amphibians", *Ed: Feng, Narins, Popper & Fay*, *New York: Springer Verlag*, pp. 113-146, (2006)

11 **Jinnai M.**, Tsuge S., Kuroiwa S., Ren F. and Fukumi M., "New similarity scale to measure the difference in like patterns with noise", *International Journal of Advanced Intelligence*, Volume 1, Number 1, pp. 59-88 (2009) http://aia-i.com/ijai/contents.html

12 Klump GM, Benedix JH, Gerhardt HC, Narins PM, "AM representation in green treefrog auditory nerve fibers: neuroethological implications for pattern recognition and sound localization", *J Comp Physiol*, 190, 1011-1021 (2004)

13 Markman S, Leitner S, Catchpole C, Barnsley S, Müller CT, Pascoe D, and Buchanan KL, "Pollutants Increase Song Complexity and the Volume of the Brain Area HVC in a Songbird", *PLoS ONE 3*, e1674 (2008)

14 Nottebohm F. and Selander RK, "Vocal Dialects and Gene Frequencies in the Chingolo Sparrow (Zonotrichia capensis)", *Condor*, 74, 137-143 (1974)

15 Nicholls JA, Goldizen AW, "Habitat type and density influence vocal signal design in satin bowerbirds", *J Anim Ecol*, 75, 549-558 (2006)

16 Patten MA, Rotenberry JT, Zuk M, "Habitat selection, acoustic adaptation, and the evolution of reproductive isolation", *Evolution*, 58, 2144-2155 (2004)

17 Payne RB., "Ecological Consequences of Song Matching: Breeding Success and Intraspecific Song Mimicry in Indigo Buntings", *In: Natural selection and social behavior*, pp. 108-120, Chiron Press (1981)

18 Robertson, J. G. M., "Female choice, male strategies and the role of vocalizations in the Australian frog Uperoleia rugosa", *Anim Behav*, 34, 773-784 (1986)

19 Rothstein SI, Fleischer RC., "Vocal Dialects and Their Possible Relation to Honest Status Signalling in the Brown-Headed Cowbird", *Condor*, 89, 1-23 (1987)

20 Scheuber H, Jacot A, Brinkhof MW, "A potential resolution to the lek paradox through indirect genetic effects", *Proc Biol Sci*, 271, 2453-2457 (2004)

21 Seddon N, Merrill RM, Tobias JA, "Sexually Selected Traits Predict Patterns of Species Richness in a Diverse Clade of Suboscine Birds", *Am Nat*, 171, 620-631 (2008)

22 Simmons, L.W., "Genotypic variation in calling song and female preferences of the field cricket Teleogryllus oceanicus", *Anim Behav*, 68, 313-322 (2004)

23 Simmons, L.W., Zuk, M. & Rotenberry, J.T., "Geographic Variation in Female Preference Functions and Male Songs of the Field Cricket Teleogryllus oceanicus", *Evolution*, 55, 1386-1394 (2001)

24 Simmons, L.W., Zuk, M. & Rotenberry, J.T., "Immune function reflected in calling song characteristics in a natural population of the cricket Teleogryllus commodus.", *Anim Behav*, 69, 1235-1241 (2005)

25 Slabbekoorn H, Smith TB, "Bird song, ecology and speciation", *Philos Trans R Soc Lond B Biol Sci*, 357, 493-503 (2002)

26 Tregenza, T., Simmons, L.W., Wedell, N. & Zuk, M., "Female preference for male courtship song and its role as a signal of immune function and condition", *Anim Behav*, 72, 809-818 (2006)

27 Zuk, M. Rotenberry, J.T. & Simmons, L.W., "Geographical variation in calling song of the field cricket Teleogryllus oceanicus: the importance of spatial scale", *J Evol Biol*, 14, 731-741 (2001)